A Structural and Magnetic Investigation of the Inversion Degree in Spinel $NiFe_2O_4$, $ZnFe_2O_4$ and $Ni_{0.5}Zn_{0.5}Fe_2O_4$ Ferrites Prepared by Soft Mechanochemical Synthesis

Z. Ž. Lazarević, D. L. Sekulić, V. N. Ivanovski, N. Ž. Romčević

Abstract—$NiFe_2O_4$ (nickel ferrite), $ZnFe_2O_4$ (zinc ferrite) and $Ni_{0.5}Zn_{0.5}Fe_2O_4$ (nickel-zinc ferrite) were prepared by mechanochemical route in a planetary ball mill starting from mixture of the appropriate quantities of the $Ni(OH)_2/Fe(OH)_3$, $Zn(OH)_2/Fe(OH)_3$ and $Ni(OH)_2/Zn(OH)_2/Fe(OH)_3$ hydroxide powders. In order to monitor the progress of chemical reaction and confirm phase formation, powder samples obtained after 25 h, 18 h and 10 h of milling were characterized by X-ray diffraction (XRD), transmission electron microscopy (TEM), IR, Raman and Mössbauer spectroscopy. It is shown that the soft mechanochemical method, i.e. mechanochemical activation of hydroxides, produces high quality single phase ferrite samples in much more efficient way. From the IR spectroscopy of single phase samples it is obvious that energy of modes depends on the ratio of cations. It is obvious that all samples have more than 5 Raman active modes predicted by group theory in the normal spinel structure. Deconvolution of measured spectra allows one to conclude that all complex bands in the spectra are made of individual peaks with the intensities that vary from spectrum to spectrum. The deconvolution of Raman spectra allows to separate contributions of different cations to a particular type of vibration and to estimate the degree of inversion.

Keywords—Ferrites, Raman spectroscopy, IR spectroscopy, Mössbauer measurements.

I. INTRODUCTION

THE ideal crystal structure of cubic spinel ferrites $M^{2+}Fe^{3+}_2O^{2-}_4$ (M = Mg, Mn, Fe, Co, Ni, Zn) has a face centered cubic unit cell of 32 oxygen anions with cations in 24 of possible 96 interstitial sites: 8 tetrahedral (A-sites) (1/8 of the total tetrahedral sites number) and 16 octahedral [B-sites] (1/2 of total number) [1], [2]. Cations Fe^{3+} and M^{2+}, could be arranged in both sites: $(M^{2+}_{1-\delta}Fe^{3+}_\delta)[M^{2+}_\delta Fe^{3+}_{2-\delta}]O^{2-}_4$ and, therefore, ferrites are classified according to cations degree of inversion δ (positioning between normal ($\delta = 0$) and inverse ($\delta = 1$) extreme patterns). The space group symmetry of normal cubic spinels is $Fd3m$ [3]. The most of cubic ferrites at the nanosized scale have partially inverse (or "mixed") structure. Cubic ferrites may also contain a mixture of divalent metal ions: $M1_{1-x}M2_xFe_2O_4$. These quaternary compounds have interesting magnetic and magnetooptical properties that depend on the chemical composition (x), but are considerably affected by the cation distribution δ, also.

The ion concentration and distribution among A and B sites has a crucial influence on the material's microstructure, dielectric and magnetic properties [4]. It was referred that nano crystalline $NiFe_2O_4$, $ZnFe_2O_4$ and $Ni_{0.5}Zn_{0.5}Fe_2O_4$ were prepared by ball milling of oxide mixture [5]–[7], by co-precipitation method [8]–[10], solid-state reaction [4], by thermal decomposition/combustion [11], citrate precursor [12], citrate gel method [13], sol-gel method [14]–[16]. To the best of our knowledge, it is not referred on soft mechanochemical method of the ferrite nano powder synthesis.

The aim of this work was the synthesis of nanosized $NiFe_2O_4$, $ZnFe_2O_4$ and $Ni_{0.5}Zn_{0.5}Fe_2O_4$ ferrite by ball milling from starting hydroxide powder mixtures. According to [17], the phrase "soft mechanochemical route" will be used for the reaction of hydroxides. The characterization of nano powder ferrete samples are investigated by TEM, Raman, IR and Mössbauer spectroscopy.

II. EXPERIMENTAL

Starting materials for the soft mechanochemical synthesis of $NiFe_2O_4$, $ZnFe_2O_4$ and $Ni_{0.5}Zn_{0.5}Fe_2O_4$ samples were: Merck zinc and nickel hydroxides with 95% purity. Ferric-hydroxide was made in laboratory. NaOH solution (25% mass), made from 99% purity NaOH (Merck) was added to the $FeCl_3$ solution (25% mass), made from 99% purity $FeCl_3$ x $6H_2O$ (Merck) [18]. Obtained hydrated ferric-hydroxide (Fe $(OH)_3$ x nH_2O) in the form of dark brown precipitate was filtrated, washed with large amounts of water and dried in a vacuum desiccator. Before milling, the $Fe(OH)_3$ x nH_2O powder was heated at 105ºC for 24 h. The material prepared in this way had 99.5% $Fe(OH)_3$. It was confirmed by potentiometric redox titration.

Mechanochemical synthesis was performed in air atmosphere in planetary ball mill Fritsch Pulverisette 5. Balls-to-powder mass ratio was 20:1. The angular velocity of the

Z. Ž. Lazarević is with the Institute of Physics, University of Belgrade, Pregrevica 118, Zemun, Belgrade, Serbia (phone: +381 11 37 13 035; fax: +381 11 31 60 531; e-mail: lzorica@yahoo.com).

D. L. Sekulić is with the Faculty of Technical Sciences, University of Novi Sad, Novi Sad, Serbia (phone: +381 21 485 2538; e-mail: dalsek@uns.ac.rs).

V. N. Ivanovski is with the Institute of Nuclear Sciences Vinča, University of Belgrade, P.O. Box 522, 11001 Belgrade, Serbia (phone: +381 11 34 08 601; e-mail: valiva@vinca.rs).

N. Ž. Romčević is with the Institute of Physics, University of Belgrade, Pregrevica 118, Zemun, Belgrade, Serbia (phone: +381 11 37 13 026; fax: +381 11 31 60 531; e-mail: romcevi@ipb.ac.rs).

World Academy of Science, Engineering and Technology
International Journal of Materials and Metallurgical Engineering
Vol:9, No:8, 2015

supporting disc and vial was 32 and 40 rad s^{-1}, respectively. The powders obtained after milling were pressed into disc shaped samples with thickness of 2.0 mm and diameter 8.0 mm.

Transmission electron microscopy studies were performed using a JEOL JEM-2100F Microscope (Jeol Inc., Tokyo, Japan) with maximum acceleration voltage of 200 kV equipped with an ultra-high resolution objective lens pole piece having a point-to-point resolution of 0.19 nm, being sufficient to resolve the lattice images of nanoparticles. Electron diffraction patterns (EDP) of nanocrystals were recorded to obtain the diffraction rings with specific structure d-values and in that way verify the crystal structure.

The Raman scattering measurements of $NiFe_2O_4$, $ZnFe_2O_4$ and $Ni_{0.5}Zn_{0.5}Fe_2O_4$ nanopowder samples were performed in the backscattering geometry at room temperature in the air using a Jobin-Yvon T64000 triple spectrometer, equipped with a confocal microscope (100x) and a nitrogen-cooled charge coupled device detector (CCD). The spectra have been excited by a 514.5 nm line of Coherent Innova 99 Ar^+ - ion laser with an output power of less than 20 mW to avoid local heating due to laser irradiation. Spectra were recorded in the range from 100 cm 1 to 800 cm^{-1}.

The reflectivity measurements were carried out with a BOMMEM DA-8 spectrometer. A DTGS pyroelectric detector was used to cover the wave number range from 50 cm 1 to 700 cm^{-1}.

The Mössbauer spectra were collected at the room temperature in the transmission mode with a constant acceleration, using a 57Co/Rh source. The calibrations of spectra were done by laser. The isomer shift (IS) values were in agreement with values for a standard α-Fe foil at 300K. Least squares fits were calculated using the SITE option of the WINNORMOS software. Line width corrections were carried out by the transmission integral. The DIST/ISO option of the program, based on the histogram method, was used to perform distributions of Mössbauer's lines [19].

III. RESULTS AND DISCUSSION

The XRD - analysis of the $NiFe_2O_4$, $ZnFe_2O_4$ and $Ni_{0.5}Zn_{0.5}Fe_2O_4$ powder samples obtained after 25 h, 18 h and 10 h milling of starting hydroxide mixtures shows that the soft mechanochemical activation (i.e. milling of amorphous hydroxides) gives practically pure spinel ferrite phase.

Fig. 1 shows TEM images of $NiFe_2O_4$, $ZnFe_2O_4$ and $Ni_{0.5}Zn_{0.5}Fe_2O_4$ nano ferrites obtained after appropriate milling time with corresponding EDPs. TEM analysis revealed that all samples are composed of nanosized particles (around 20 nm). The final grain size in the $NiFe_2O_4$ (average ~ 10 nm) is about twice as large as that in the $ZnFe_2O_4$ (average ~ 20 nm), which is a consequence of different reaction paths in these two ferrite processing routes. The particles in $NiFe_2O_4$ and $ZnFe_2O_4$ samples have irregular shape and are highly agglomerated, while the particles in $Ni_{0.5}Zn_{0.5}Fe_2O_4$ sample are roundish and less agglomerated.
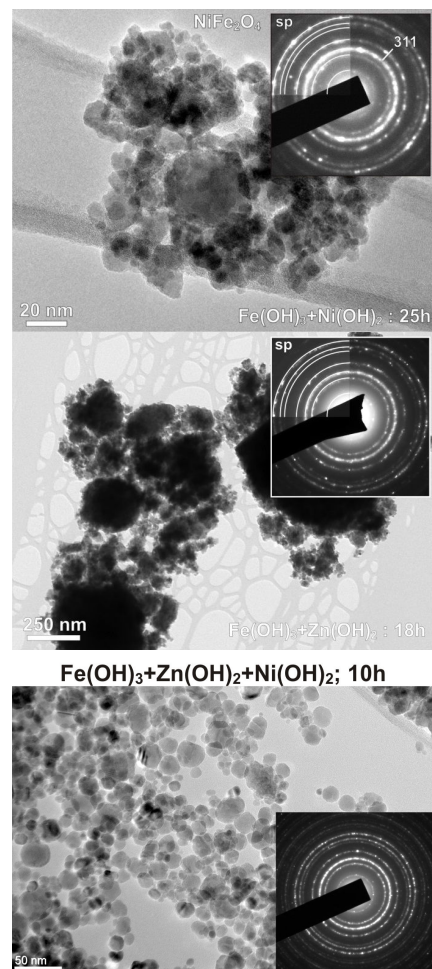

Fig. 1 TEM images with corresponding electron diffraction patterns (Debye-Sherrer rings) of $NiFe_2O_4$, $ZnFe_2O_4$ and $Ni_{0.5}Zn_{0.5}Fe_2O_4$ ferrite samples obtained from the mixture of appropriate hydroxides powders by milling for 25 h, 18 h and 10 h, respectively

A mechanochemically produced nanopowder sample of Ni0.5Zn0.5Fe2O4 ferrite has mixed spinel structure and belongs to $P4_322$ tetragonal space group [20]. However, it is usual, for the sake of simplicity, to assign Raman and IR modes as in normal cubic spinel, as the symmetry group is $Fd3m$. The factor group analysis predicts 5 Raman active modes: $A_{1g} + E_g + 3F_{2g}$ and 4 IR active modes $4F_{1u}$ from the center of Brillouin zone in the normal spinel.

It is obvious that all samples have more than 5 Raman active modes predicted by group theory in the normal spinel structure. Deconvolution of measured spectra allows one to conclude that all complex bands in the spectra are made of individual peaks with the intensities that vary from spectrum to spectrum. In order to determine the origin of the peaks, we have compared the Raman spectra of $NiFe_2O_4$ and $ZnFe_2O_4$ [21], with the spectrum of single phase $Ni_{0.5}Zn_{0.5}Fe_2O_4$, Fig. 2. On the example of single phase sample of $Ni_{0.5}Zn_{0.5}Fe_2O_4$ obtained by milling of hydroxides for 10 h it is visible that modes originated from vibrating of different cations (in $NiFe_2O_4$, or $ZnFe_2O_4$) are reproduced in Raman spectra of mixed $Ni_{0.5}Zn_{0.5}Fe_2O_4$.
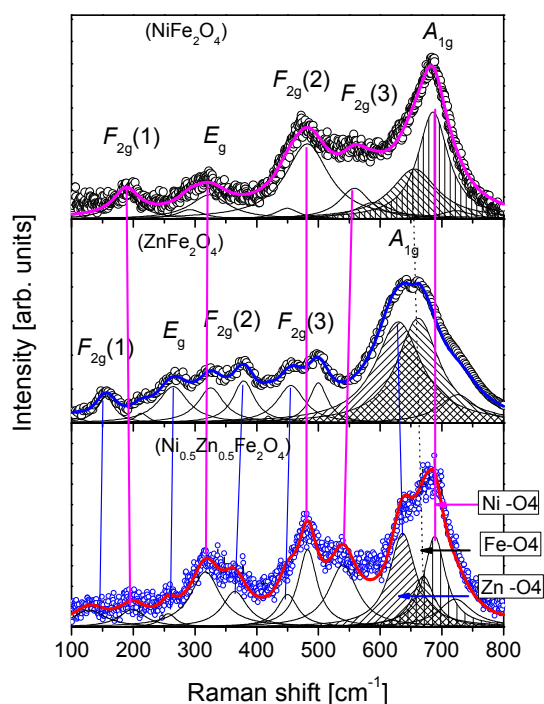
World Academy of Science, Engineering and Technology
International Journal of Materials and Metallurgical Engineering
Vol:9, No:8, 2015

Fig. 2 Raman spectra of the NiFe$_2$O$_4$, ZnFe$_2$O$_4$ and Ni$_{0.5}$Zn$_{0.5}$Fe$_2$O$_4$ ferrite samples obtained from the mixture of appropriate hydroxides powders by milling for 25 h, 18 h and 10 h, respectively

The high frequency first order mode A_{1g} is due to symmetric stretching of oxygen atoms along Zn-O, Fe-O and Ni-O bonds in the tetrahedral coordination [22]. The mode at 637 cm^{-1} is related with stretching along Zn-O bonds in tetrahedrons [23], [24]. The mode at 670 cm^{-1} is related with Fe-O bonds stretching [25], at 689 cm^{-1} with Ni-O bonds [18], [26] and a small mode at 721 cm^{-1} corresponds to A_{1g} mode of maghemite, that is to oscillations of Fe-O in uncompleted tetrahedrons (with oxygen vacancies) [27]. In principle, modes $F_{2g}(2)$ and $F_{2g}(3)$ correspond to the vibrations of the octahedral group, but it seems that components of these modes can hardly be resolved in the Raman spectra of Ni$_{0.5}$Zn$_{0.5}$Fe$_2$O$_4$. At about 370 cm^{-1} is the Zn-component of $F_{2g}(2)$ mode, at 480 cm^{-1} is Ni - $F_{2g}(2)$ and between them Zn - component of $F_{2g}(3)$ mode, Fig. 2. These modes are not very strong and the possible fitting error can be too high because of rather high level of noise. For that reason we tried to analyze the most exaggerate A_{1g} mode and to estimate the inversion parameter from the ratio of the intensities of A_{1g} components. The integrated intensity of certain component of A_{1g} mode is proportional approximately to the contribution of the corresponding cations in A-sites. The participation of Zn^{2+} in A-sites should be: xZn(A) = I$_{Zn}$ /(I$_{Zn}$ + I$_{Ni}$ +I$_{Fe}$ + I$_{Fe*}$). In the exact formula intensities of Lorentzians are multiplied by corresponding force constants. We can suppose that the force constant in the case of "maghemite" oscillation is much smaller than the force constants of other vibrations (in regular surrounding) and to neglect its contribution. In this approximation, for hydroxide sample, Fig. 2, we obtained:

Fe$_{0.20}$Ni$_{0.35}$Zn$_{0.44}$, what is roughly like the result of Rietveld analysis (Rietveld analysis gives: Fe$_{0.17}$Ni$_{0.31}$Zn$_{0.48}$).
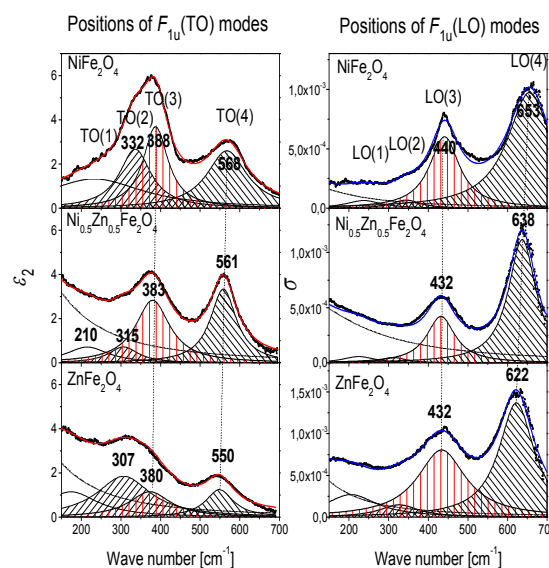

Fig. 3 Comparison of the results of Kramers-Krönig analysis of IR spectra of NiFe$_2$O$_4$, ZnFe$_2$O$_4$ and Ni$_{0.5}$Zn$_{0.5}$Fe$_2$O$_4$ ferrites

In Fig. 3 are compared the results of Kramers-Krönig analysis of three FIR spectra: NiFe$_2$O$_4$, ZnFe$_2$O$_4$ and mixed Ni$_{0.5}$Zn$_{0.5}$Fe$_2$O$_4$ ferrite. It is visible that the positions of both TO and LO modes shift to lower wave numbers with increasing of total mass of divalent cations. Considering that in literature could be found various values of frequencies even for sintered ferrites, we cannot expect accurate estimation of cation distribution in nanopowders on the basis of FIR measurements. However, there is no doubt that FIR technique could show the presence of small amounts of unreacted starting compounds.

The Mössbauer spectra show distributions of hyperfine fields. In order to investigate valence and coordination number (CN) of iron cations in the spinel, distributions are partitioned on disjunct subspectra based on Lorentzian lines.

The Mössbauer spectrum (Fig. 4 (a)) of NiFe$_2$O$_4$ consists of nine subspectra, precisely seven sextets and two doublets. According to the Mössbauer parameters, the sextets are divided in three types marked with letter L, M, and S. The sextets marked with L represent resonance response of ion 57Fe from the large NiFe$_2$O$_4$ nanoparticles. The existence of magnetic ions on both (A) and [B] sites allows three types of antiferromagnetic exchange interactions: (A)-(A), (A)-[B], and [B]-[B]. The strongest interactions, according to the Weiss model, are between Ni^{2+} or Fe^{3+} ions at tetrahedral sites and Fe^{3+} ions at the octahedral sites [28].

The Mössbauer spectroscopy of 25 h milled mixture Fe(OH)$_3$/Ni(OH)$_2$ reveals that more of 90% emergent iron containing powder, is in the NiFe$_2$O$_4$ phase. Using a formula [A$_{(A)}$/A$_{[B]}$ = f$_{(A)}$/f$_{[B]}$×δ/(2-δ)], where A is area of subspectrum, and assuming that the ratio of the recoil-less fraction is f$_{[B]}$/f$_{(A)}$ = 0.94 at the room temperature, one could obtain δ [29]–[30].

World Academy of Science, Engineering and Technology
International Journal of Materials and Metallurgical Engineering
Vol:9, No:8, 2015

According to the areas of measured sextets, only for large size particles, the estimated value for the degree of inversion is 70%, with uncertainty of 40%.

The Mössbauer spectrum taken from 18 h milled $Zn(OH)_2/Fe(OH)_3$ sample consists of three sextets and three doublets (Fig. 4 (b)). The parameters of one sextet with relative abundance of 2.9% refer on the presence of α-Fe. The resonant signals make sextets having the origin from iron ions on tetrahedral sites. On the other side, the doublets are created by signals from octahedral standing iron ions. For this sample, the inversion parameter δ is 0.58(63). The δ is calculated by data, based on followed total fitted area: A(A) = 56(32) and A[B] = 41.1(18.7).

The Mössbauer spectrum of the sample obtained from the mixture of $Ni(OH)_2/Zn(OH)_2/Fe(OH)_3$ powders after 10 h of milling is fitted by 10 sextets, two superparamagnetic doublets and two singlet (Fig. 4 (c)). Two sextets with the smallest isomer shift are referred to tetrahedral A-site with different occupation numbers and the other sextets are referred to B-site surrounded with different number of magnetic ions or disturbed in other way. Two doublets (SPD), with high isomer shift, could be connected with Fe^{3+} ions in very small superparamagnetic nanoparticles. There are also two superparamagnetic singlets (SPS), which could be assigned to the tetrahedral (SPSA) and to the octahedral (SPSB) site. All subspectra correspond to the pure spinel ferrite phase. We find that the degree of inversion estimated for the single phase nickel-zinc ferrite sample obtained during 10 h milling of starting hydroxides is $\delta = 0.36(3)$. The presented analysis of the Mössbauer spectra of the $Ni_{0.5}Zn_{0.5}Fe_2O_4$ sample is in good agreement with conclusions of previous measurements (XRD, EDP, EDS, Raman and IR).
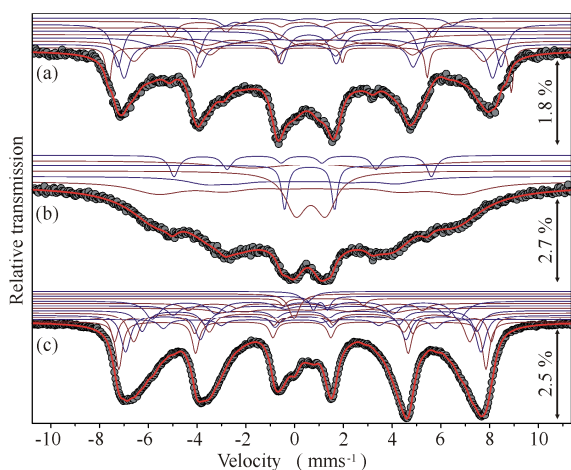

Fig. 4 Mössbauer spectra of (a) $NiFe_2O_4$, (b) $ZnFe_2O_4$ and (c) $Ni_{0.5}Zn_{0.5}Fe_2O_4$ ferrite samples obtained from the mixture of appropriate hydroxides powders by milling for 25 h, 10 h and 18 h, respectively

IV. Conclusion

It is important to emphasize that the aim of this study is to show that under the laboratory conditions, it is simple to prepare the good quality nanosized $NiFe_2O_4$, $ZnFe_2O_4$ and $Ni_{0.5}Zn_{0.5}Fe_2O_4$ ferrite powders by soft mechanochemical synthesis. It was examined evolution of the synthesis of nano ferrites starting from the appropriate mixtures of powders milled in different duration time. The starting materials were: mixture of $Ni(OH)_2/Fe(OH)_3$, $Zn(OH)_2/Fe(OH)_3$ $Ni(OH)_2/Zn(OH)_2/Fe(OH)_3$ hydroxide powders. The $NiFe_2O_4$, $ZnFe_2O_4$ and $Ni_{0.5}Zn_{0.5}Fe_2O_4$ ferrite obtained by milling after 25 h, 18 h and 10 h, respectively. These samples are compared and investigated using various characterization methods. X-ray diffraction of the obtained samples shows single phase cubic spinel structure. TEM analysis revealed that all samples are composed of agglomerated nanosize particles (on average ≈ 20 nm). In the Raman and IR spectra are observed all of first-order Raman and IR active modes. In the Raman spectra of $Ni_{0.5}Zn_{0.5}Fe_2O_4$ modes originated from vibrating of different cations (Ni-ferrite-like, Zn-ferrite-like, or magnetite-like) are clearly visible. The degree of the cation inversion of $Ni_{0.5}Zn_{0.5}Fe_2O_4$ is estimated for spinel fraction in all samples. The Mössbauer spectra of samples were fitted by several subspectra and according to known subspectral areas of both iron sites the degree of inversion was calculated. In the case of single phase $Ni_{0.5}Zn_{0.5}Fe_2O_4$ sample obtained from the mixture of appropriate hydroxide powders for 10 h milling the cation inversion is $\delta = 0.36(3)$.

References

[1] M. Mohapatra, and S. Anand, "Synthesis and applications of nano-structured iron oxides/hydroxides – a review," *International Journal of Engineering, Science and Technology*, vol. 2, no. 8, pp. 127–146, Xxx. 2010, www.ijest-ng.com.

[2] A. R. Tanna, and H. H. Joshi, "Computer aided X-ray diffraction intensity analysis for spinels: hands-on computing experience," *World Academy of Science, Engineering and Technology*, vol. 7, no.3, pp. 70–77, 2013.

[3] W. H. Bragg, "The structure of magnetite and the spinels" *Nature*, Lond. vol. 95, pp. 561, 1915.

[4] Q. Liu, L. Lv, J. P. Zhou, X. M. Chen, X. B. Bian, and P. Liu, "Influence of nickel-zinc ratio on microstructure, magnetic and dielectric properties of $Ni_{(1−x)}Zn_xFe_2O_4$ ferrites," *Journal of Ceramic Processing Research*, vol. 13, no. 2, pp. 110–116, 2012.

[5] Č. Jovalekić, M. Zdujić, A. Radaković, and M. Mitrić, "Mechanochemical synthesis of $NiFe_2O_4$ ferrite," *Materials Letters*, vol. 24, no.6, pp. 365–368, 1995.

[6] C. N. Chinnasamy, A. Narayanasamy, N. Ponpandian, K. Chattopadhyay, H. Guerault, and J. M. Greneche, "Ferrimagnetic ordering in nanostructured zinc ferrite," *Scripta Materialia*, vol. 44, no. 8–9, pp. 1407–1410, 2001.

[7] M. Jalaly, M. H. Enayati, and F. Karimzadeh, "Investigation of structural and magnetic properties of nanocrystalline $Ni_{0.3}Zn_{0.7}Fe_2O_4$ prepared by high energy ball milling," *Journal of Alloys and Compounds*, vol. 480, pp. 737–740, 2009.

[8] K. Maaz, A. Mumtaz, S. K. Hasanain, and M. F. Bertino, "Temperature dependent coercivity and magnetization of nickel ferrite nanoparticles," *Journal of Magnetism and Magnetic Materials*, vol. 322, no.15, pp. 2199–2202, 2010.

[9] P. Sivakumar, R. Ramesh, A. Ramanand, S. Ponnusamy, and C. Muthamizhchelvan, "Synthesis and characterization of $NiFe_2O_4$ nanosheet via polymer assisted co-precipitation method," *Materials Letters*, vol. 65, no. 3, pp. 483–485, 2011.

World Academy of Science, Engineering and Technology
International Journal of Materials and Metallurgical Engineering
Vol:9, No:8, 2015

[10] E. Manova, D. Paneva, B. Kunev, E. Rivière, C. Estournès, and I. Mitov, "Characterization of nanodimensional Ni-Zn ferrite prepared by mechanochemical and thermal methods," *Journal of Physics: Conference Series*, vol. 217, no. 1, pp. 012102, 2010, doi:10.1088/1742-6596/217/1/012102.

[11] K. Suresh, and K. C. Patil, "Preparation and properties of fine particle nickel-zinc ferrites: A comparative study of combustion and precursor methods," *Journal of Solid State Chemistry*, vol. 99, no. 1, pp. 12–17, 1992.

[12] A. Verma, T. C. Goel, and R. G. Mendiratta, "Low temperature processing of NiZn ferrite by citrate precursor method and study of properties," *Materials Science and Technology*, vol. 16, pp. 712–715, 2000.

[13] K. R. Krishna, K. V. Kumar, C. Ravindernath Gupta, and D. Ravinder, "Magnetic properties of Ni-Zn ferrites by citrate gel method," *Advances in Materials Physics and Chemistry*, vol. 2, no. 3, pp. 149–154, 2012, http://dx.doi.org/10.4236/ampc.2012.23022.

[14] A. T. Raghavender, K. Zadro, D. Pajic, Z. Skoko, and N. Biliskov, "Effect of grain size on the Néel temperature of nanocrystalline nickel ferrite," *Materials Letters*, vol. 64, no. 10, pp. 1144–1146, 2010.

[15] H. E. Zhang, B. F. Zhang, G. F. Wang, X. H. Dong, and Y. Gao, "The structure and magnetic properties of $Zn_{1-x}Ni_xFe_2O_4$ ferrite nanoparticles prepared by sol–gel auto-combustion," *Journal of Magnetism and Magnetic Materials*, vol. 312, pp. 126–130, 2007.

[16] A. T. Raghavender, N. Biliškov, and Ž. Skoko, "XRD and IR analysis of nanocrystalline Ni–Zn ferrite synthesized by the sol–gel method," *Materials Letters*, vol. 65, pp. 677–680, 2011.

[17] E. Avvakumov, M. Senna, and N. Kosova, Soft Mechanochemical Synthesis: A Basis for New Chemical Technologies, Kluwer Academic Publishers, Boston, 2001.

[18] Z. Ž. Lazarević, Č. Jovalekić, A. Rečnik, V. N. Ivanovski, A. Milutinović, M. Romčević, M. B. Pavlović, B. Cekić, and N. Ž. Romčević, "Preparation and characterization of spinel nickel ferrite obtained by the soft mechanochemically assisted synthesis," *Materials Research Bulletin*, vol. 48, pp. 404–415 , 2013.

[19] R. A. Brand, WinNormos Mössbauer fitting program, Universität Duisburg, 2008.

[20] Ivanov, M. V. Abrashev, M. N. Iliev, M. M. Gospodinov, J. Meen, and M. I. Aroyo, "Short-range B-site ordering in the inverse spinel ferrite $NiFe_2O_4$," *Physical Review B*, vol. 82, pp. 024104, 2010, http://dx.doi.org/10.1103/PhysRevB.82.024104.

[21] Z. Ž. Lazarević, Č. Jovalekić, A. Milutinović, D. Sekulić, V. N. Ivanovski, A. Rečnik, B. Cekić, and N. Z. Romčević, "Nanodimensional spinel $NiFe_2O_4$ and $ZnFe_2O_4$ ferrites prepared by soft mechanochemical synthesis," *Journal of Applied Physics*, vol. 113, pp. 187221, 2013.

[22] Z. W. Wang, P. Lazor, S. K. Saxena, and G. Artioli, "High-pressure Raman spectroscopic study of spinel ($ZnCr_2O_4$)," *Journal of Solid State Chemistry*, vol. 165, 165–170, 2002.

[23] M. Maletin, E. G. Moshopoulou, A. G. Kontos, E. Devlin, A. Delimitis, V. T. Zaspalis, L. Nalbandian, and V. V. Srdić, "Synthesis and structural characterization of In-doped $ZnFe_2O_4$ nanoparticles," *Journal of the European Ceramic Society*, vol. 27, pp. 4391–4394, 2007.

[24] A. Milutinović, Z. Ž. Lazarević, Č. Jovalekić, I. Kuryliszyn-Kudelska, M. Romčević, S. Kostic, and N. Ž. Romčević, "The cation inversion and magnetization in nanopowder zinc ferrite obtained by soft mechanochemical processing," *Materials Research Bulletin*, vol. 48, pp. 4759–4768, 2013.

[25] O. N. Shebanova, and P. Lazor, "Raman study of magnetite (Fe_3O_4): laser-induced thermal effects and oxidation," *Journal of Raman Spectroscopy*, vol. 34, pp. 845–852, 2003.

[26] A. Ahlawat, and V. G. Sathe, "Raman study of $NiFe_2O_4$ nanoparticles, bulk and films: effect of laser power," *Journal of Raman Spectroscopy*, vol. 42, pp. 1087–1094, 2011.

[27] Ž. Cvejić, S. Rakić, A. Kremenović, B. Antić, Č. Jovalekić, and P. Colomban, "Nanosize ferrites obtained by ball milling: crystal structure, cation distribution, size-strain analysis and Raman investigations," *Solid State Sciences*, vol. 8, no. 8, pp. 908–915, 2006.

[28] N. N. Greenwood, and T. C. Gibb, Mössbauer Spectroscopy, Chapman and Hall Ltd., London, pp. 266–267, 1971.

[29] V. Šepelák, D. Baabe, and K. D. Becker, "Mechanically induced cation redistribution and spin canting in nickel ferrite," *Journal of Materials Synthesis and Processing,* vol. 8, no. 5-6, pp. 333–337 (2000).

[30] G. A. Sawatzky, F. Van der Woude, and A. H. Morrish, "Mössbauer study of several ferrimagnetic spinel," *Physical Review*, vol. 187, no.2, 747–757, 1969.